

**A Natural Gas to Liquids (GTL) Process Model for
Optimal Operation**

Journal:	<i>Industrial & Engineering Chemistry Research</i>
Manuscript ID:	ie-2011-014058.R1
Manuscript Type:	Article
Date Submitted by the Author:	n/a
Complete List of Authors:	Panahi, Mehdi; NTNU, Chemical Engineering Rafiee, Ahmad; NTNU, Chemical Engineering Skogestad, Sigurd; NTNU, Chemical Engineering Hillestad, Magne; NTNU, Chemical Engineering

SCHOLARONE™
Manuscripts

A Natural Gas to Liquids (GTL) Process Model for Optimal Operation

Mehdi Panahi, Ahmad Rafiee, Sigurd Skogestad* and Magne Hillestad

Department of Chemical Engineering, Norwegian University of Science and Technology (NTNU), 7491

Trondheim, Norway

Abstract

The design and optimization of a natural gas to hydrocarbon liquids (GTL) process is considered, mainly from the view of maximizing the variable income during operation. Auto-thermal reforming (ATR) is used for synthesis gas production. The kinetic model for Fischer-Tropsch (FT) reactions is the one given by Iglesia et al. for a Cobalt based FT reactor. For the product distribution, three alternative expressions for the chain growth factor α are compared.

Keywords

Fischer-Tropsch (FT), Chain growth probability, Auto-thermal reforming (ATR), Slurry bubble column reactor (SBCR), Simulation, Optimization, Degrees of freedom, Active constraints

1. Introduction

A GTL (gas to liquids) plant consists of three main sections (Figure 1): Synthesis gas production, Fischer-Tropsch (FT) reactor and FT products upgrading¹. In this process, natural gas is first converted to synthesis gas (“syngas”; a mixture of hydrogen and carbon monoxide) which is further converted to a range of hydrocarbons in an FT reactor.

*Corresponding author. Tel.: +47 73594154; fax.: +47 73594080
E-mail address: skoge@ntnu.no

There are different routes for syngas production: auto-thermal reforming (ATR), steam reforming, combined reforming and gas heated reforming². We have considered ATR which to be claimed the most economical route for syngas production^{3,4}.

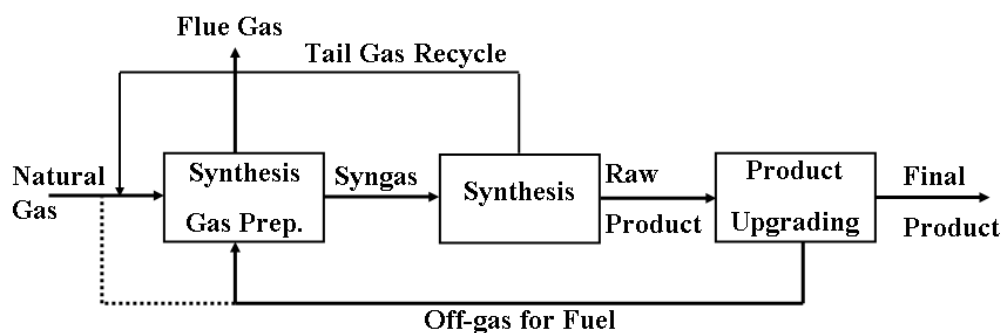


Fig. 1- A simple Flowsheet of a GTL process¹

FT reactions can take place on either iron or Cobalt catalysts in four different types of reactor²; fixed bed, slurry bubble column (SBCR), fluidized bed and circulating fluidized bed reactor.

The currently largest operating GTL plant is the Oryx plant in Qatar with a production capacity of 34,000 bbl/day liquid fuels. This plant includes two parallel trains with two Cobalt based slurry bubble column reactors, each with the capacity of 17,000 bbl/day operating at low temperature FT conditions. Shell is also commissioning a world scale GTL plant (Pearl GTL plant) in 2011 with the capacity of 260,000 bbl/day; 120,000 bbl/day upstream products and 140,000 bbl/day GTL products⁵. This plant is located close to Oryx GTL plant. Shell uses fixed bed reactor for the FT synthesis. Pearl GTL plant has 24 parallel fixed bed reactors each with the production capacity of 6,000 bbl/day⁶.

In the current study, based on available information in open literatures, we study a single train with a capacity of approximately 17,000 bbl/day. The natural gas feed condition is

1
2
3 assumed to be fixed at 8195 kmol/h (164.2 MMSCFD), 3000 kPa and 40°C. The
4
5 composition of natural gas in mole basis is:
6
7

- 8 – CH₄: 95.5%
- 9 – C₂H₆: 3%
- 10 – C₃H₈: 0.5%
- 11 – n-C₄H₁₀: 0.4%
- 12 – N₂: 0.6%
- 13
- 14
- 15

16 The upgrading section is not included. The main objective of this work is to develop a
17 detailed model that gives the effect of the main operational decision variables on the
18 variable income while satisfying operational constraints. The decision variables include
19 the H₂O to hydrocarbon feed ratio to the pre-reformer, the Oxygen to hydrocarbon feed
20 ratio to the ATR, the recycle tail gas fraction to the syngas and FT reactors, the purge
21 fraction and the CO₂ removal fraction. The UniSim commercial process simulator⁷ is
22 used to simulate the process. The simulator uses detailed steady-state mass and energy
23 balances, and we chose to use the SRK equation of state for the thermodynamic
24 properties. The UniSim files are available from the authors.
25
26
27
28
29
30
31
32
33
34
35
36

37 Another modeling and simulation study for a GTL plant was recently published by Bao et
38 al⁸ where the focus is on optimal process design. They assume a fixed value for the
39 H₂/CO ratio of 2 and a fixed chain growth probability (α) for the FT reactions. On the
40 other hand, our focus is on optimal operation, and our model allows for varying
41 (optimized) H₂/CO ratio and uses a model with varying α .
42
43
44
45
46
47
48
49

50 **2. Modeling and process description**

51 The overall flowsheet for the process studied is shown in Figure 2.
52
53
54
55
56
57
58
59
60

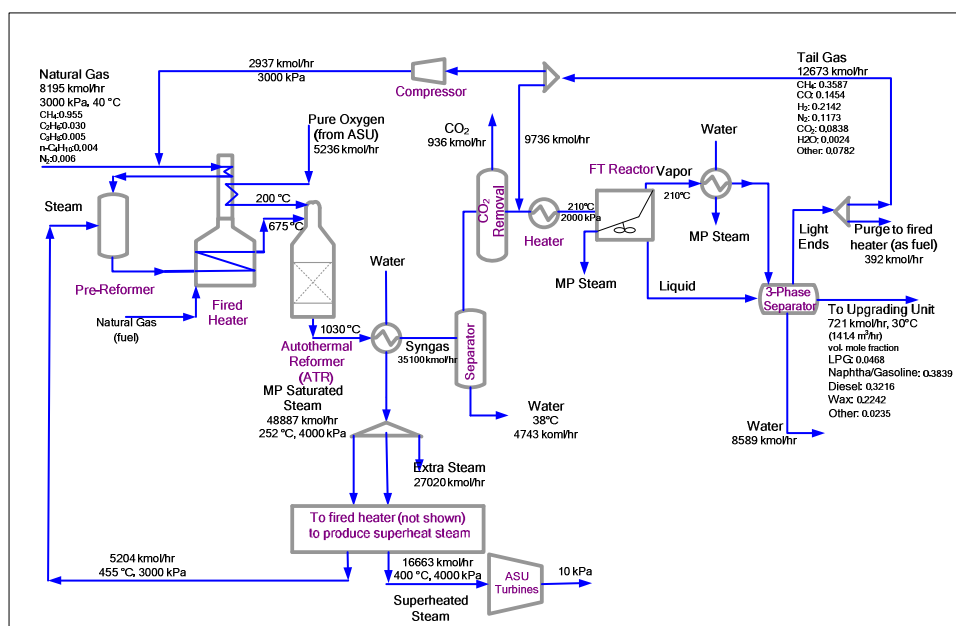
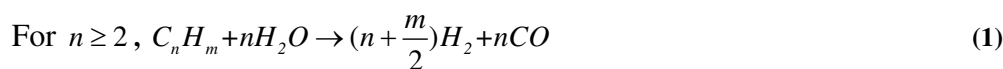


Fig. 2- Overall process flowsheet with final optimized data (α_2 model, wax price=0.63 USD/kg)

2.1. The synthesis gas section

The syngas part is similar to the configuration proposed by Haldor Topsøe³ with operating pressure of 3000 kPa and includes a pre-reformer, a fired heater and a ATR:

1. The pre-reformer is used to avoid cracking of heavier hydrocarbons in the subsequent ATR. It is assumed that all hydrocarbons heavier than methane are converted according to eq.(1). In addition, the methanation and shift reactions (eq.(2) and eq.(3)) are assumed to be in equilibrium^{3,9}. In our case, the reactor is assumed to be adiabatic with the feed entering at 455°C¹⁰. The reaction scheme is



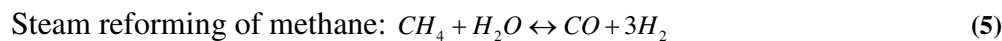
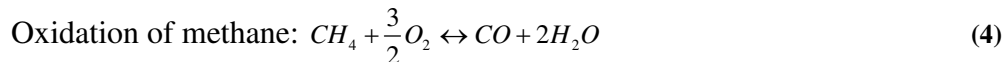
The exit temperature of the adiabatic pre-reformer will depend on the inlet composition and temperature. The exit temperature is between 100 and 300°C lower than the desired ATR inlet temperature, which means that a fired heater is needed.

2. The fired heater is used to supply the required energy for:

- 1
2
3
4
5
6
7
8
9
10
11
12
13
14
15
16
17
18
19
20
21
22
23
24
25
26
27
28
29
30
31
32
33
- a) Preheating the following streams to 455°C:
 - fresh natural gas (pre-reformer feed)
 - recycle hydrocarbons from FT reactor (pre-reformer feed)
 - b) Superheated process steam (pre-reformer feed) and superheated steam for driving the turbines of compressor in the oxygen plant and the much smaller recycled tail gas compressor. Note that saturated steam is first produced in a boiler by heat exchange with the hot outlet stream of the ATR and is then superheated in the fired heater. The energy consumption in the oxygen plant is assumed $400 \frac{\text{kWh}}{\text{ton O}_2}^{10}$. This power is supplied by superheated steam from the fired heater, which is expanded from 400 bar and 400°C to 0.1 bar in the ASU turbine (75% efficiency assumed).
 - c) Preheating the outlet gas from the pre-reformer to 675°C (optimized value, see below)
 - d) Preheating oxygen to 200°C³
 - e) 10% of the total fired heater duty is assumed to be used to supply superheated steam for other mechanical equipment in the process.

34 The required fuel for the fired heater is supplied by the combustible components in
35 the purge stream plus some fresh natural gas. An efficiency of 98% is assumed for the
36 combustion of fuels¹¹.
37
38
39

40
41 3. The ATR converts methane in the stream from the fired heater to syngas by
42 reacting it with steam and oxygen. It is modeled as an adiabatic equilibrium
43 reactor according to the following reactions¹¹;
44
45
46



1
2
3 The oxygen is supplied by the air separation unit (ASU) and is blown into the ATR. For
4
5
6
7
8
9
10
11
12
13
14
15
16
17
18
19
20
21
22
23
24
25
26
27
28
29
30
31
32
33
34
35
36
37
38
39
40
41
42
43
44
45
46
47
48
49
50
51
52
53
54
55
56
57
58
59
60

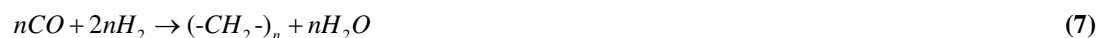
The oxygen is supplied by the air separation unit (ASU) and is blown into the ATR. For GTL applications with a Cobalt based Fischer Tropsch reactor, a typical H₂ to CO ratio in the fresh syngas is about 2³, but the exact value will be obtained as a part of the optimization of the process. The hot syngas leaving the ATR is cooled down to ambient temperature for water removal before going to the CO₂ capture unit.

Note that large amounts of water is produced in the subsequent FT reactor, so there is no strict limitation on the water content of cooled syngas, but it is removed for economic reasons to reduce the flow to the FT reactor. The CO₂ removal plant is modeled as a component splitter, where only CO₂ is removed.

With our natural gas feed rate, the hot syngas from the ATR is used to produce about 49000 kmol/hr medium pressure saturated steam (40bar, 252°C) in the boiler. 34% of this MP steam is superheated in the fired heater to be used in the Oxygen plant, and 11% is superheated in the fired heater to be used as the process steam into the pre-reformer. The remaining “extra” 55% of the saturated steam is a byproduct of the plant (These values correspond to the optimal model mentioned further in Table 5).

2.2. Fischer Tropsch section

The syngas is sent to the Fischer-Tropsch (FT) reactor where the highly exothermic FT reactions take place¹³. The reactor is assumed isothermal with a temperature of 210°C (483K). The reactions are typically written in the following form



where $(-CH_2)_n$ denote the olefin and paraffin main products. In addition, CH₄ formation is unavoidable



The FT product distribution can be described by the well known Anderson-Schulz-Flory (ASF) model

$$w_n = n(1-\alpha)^2 \alpha^{n-1} \quad (9)$$

where w_n ($n>1$) is the weight fraction of C_n and α is chain growth probability. The water- gas shift reaction is negligible because it is not catalyzed on Cobalt catalyst¹³.

Figure 3 illustrates the meaning of the chain growth graphically. The probability of chain termination is $1-\alpha$. Three different methods for calculating the chain growth probability α are described in section 3. To simulate the reaction scheme, we use the reaction rates for CO consumption and CH₄ formation proposed by Iglesia et al.¹⁴ together with the carbon mass balance as given by the ASF distribution model. (see Appendix for details).

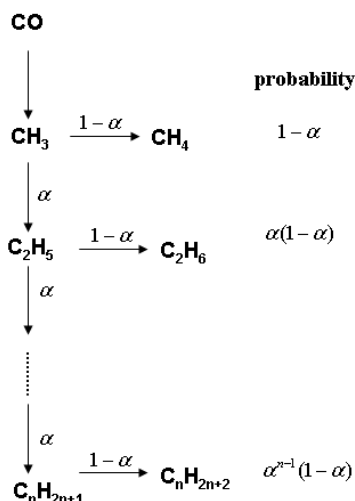


Fig. 3- Probability of chain growth to different hydrocarbons in FT reactions⁶

Iglesia's reaction rates on Cobalt catalyst are valid at 473 to 483 K, 100 to 3000 kPa, H₂/CO=1-10, and described as below.

$$r_{\text{CH}_4} = \frac{7.334 \times 10^{-10} P_{\text{H}_2} P_{\text{CO}}^{0.05}}{1 + 3.3 \times 10^{-5} P_{\text{CO}}} \left(\frac{\text{kmol}_{\text{CH}_4}}{m_{\text{reactor}}^3 \cdot \text{s}} \right) \quad (10)$$

$$r_{\text{CO}} = \frac{1.331 \times 10^{-9} P_{\text{H}_2}^{0.6} P_{\text{CO}}^{0.65}}{1 + 3.3 \times 10^{-5} P_{\text{CO}}} \left(\frac{\text{kmol}_{\text{CO}}}{m_{\text{reactor}}^3 \cdot \text{s}} \right) \quad (11)$$

where pressure is in Pa.

1
2
3 The simulated reactor is a slurry bubble column reactor (SBCR), which is well-known for
4 good heat removal. The following lumps are defined as FT products in our model¹⁵: C₁,
5 C₂, LPG (C₃-C₄), Gasoline/Naphtha (C₅-C₁₁), Diesel (C₁₂-C₂₀) and Wax (C₂₁₊). Note that
6 for each carbon number, both olefins and paraffins are produced and the factor γ
7 determines the olefins/paraffins ratio (see Appendix for details).
8
9

10 An equilibrium three-phase separator operating at 38°C and 20 bar is used for the FT
11 products separation. As for the other units, the SRK equation of state is used for the
12 thermodynamic equilibrium. In all cases, the H₂O mole fraction in the raw product (outlet
13 hydrocarbon stream of the separator) is less than 0.07% .
14
15

16 The pressure drop in the individual equipment of the syngas and FT units is ignored. This
17 assumption has the same effect on all the three alpha-cases, because the relative change
18 of objective function in different price scenario is important and not the absolute value.
19
20
21
22
23
24

25 **3. Calculation of chain growth probability α**

26 Three different methods for obtaining α have been considered. Note that in all cases, the
27 ASF model using α is applied for $n>1$, whereas methane ($n=1$) is found from the
28 reaction rate by Iglesias.
29
30
31
32

33 **3.1. Using rates of Iglesia (α_i)**

34 From the proposed reaction rates for CO (eq. (10)) and CH₄ (eq. (11)), the selectivity of
35 CH₄ as a function of partial pressures of H₂ and CO in FT reactor can be found (left hand
36 side of eq.(12)). Next, from (A-9) in the Appendix, the selectivity, $\frac{r_{CH_4}}{r_{CO}}$ can be found as a
37 function of α (right hand side of eq. (12)).
38
39
40
41
42
43
44
45
46
47
48
49
50
51
52
53
54
55
56
57
58
59
60

$$\frac{r_{CH_4}}{r_{CO}} = 0.55 \frac{P_{H_2}^{0.4}}{P_{CO}^{0.6}} = \frac{w_1 \times 2000}{16 \times \left[\frac{w_1}{16} + 2w_2 \left(\frac{1}{1+\gamma} \frac{1}{30} + \frac{\gamma}{1+\gamma} \frac{1}{28} \right) + \dots + 25w_{25} \left(\frac{1}{1+\gamma} \frac{1}{352} + \frac{\gamma}{1+\gamma} \frac{1}{350} \right) \right]}{(1-\alpha)^2 \times 2000} = \frac{16 \times \left[\frac{(1-\alpha)^2}{16} + 2(2\alpha(1-\alpha)^2) \left(\frac{1}{1+\gamma} \frac{1}{30} + \frac{\gamma}{1+\gamma} \frac{1}{28} \right) + \dots + 25(1-2\alpha-3\alpha^2-\dots-20\alpha^{19})(1-\alpha)^2 \left(\frac{1}{1+\gamma} \frac{1}{352} + \frac{\gamma}{1+\gamma} \frac{1}{350} \right) \right]}{(1-\alpha)^2 \times 2000} \quad (12)$$

In spite of the complicated appearance of eq.(12), it can be easily solved for α . We call this solution α_1 in the rest of the paper. From its definition, α is in the range of [0,1] and interestingly eq.(12) has only one real root in this range. Figure 4 shows the value of the real roots for a wide range of variation in the selectivity. Out of 19 roots, 16 are always imaginary and 2 out of 3 real ones are always greater than 1.

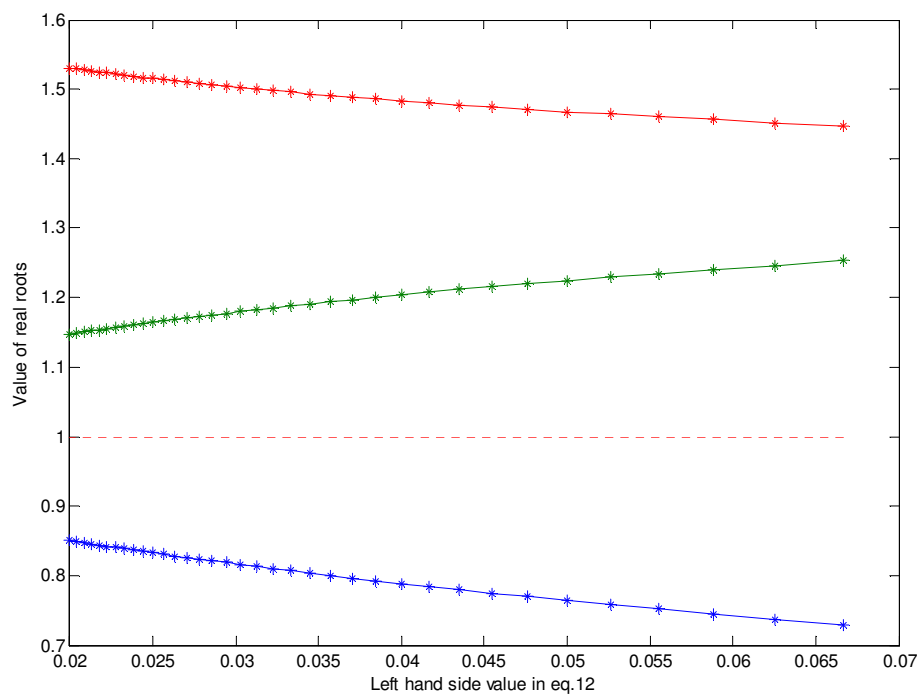


Fig. 4- Real roots α as a function of the selectivity ($1.2 \leq H_2/CO \leq 2.15$)

3.2. Using modified function of Yermakova and Anikeev (α_2)

The following function has been proposed by Yermakova and Anikeev¹⁶ and modified by Song et al.¹⁷

$$\alpha = (0.2332 \frac{y_{CO}}{y_{CO} + y_{H_2}} + 0.633)[1 - 0.0039(T - 533)] \quad (13)$$

Here y_{CO} and y_{H_2} are mole fractions in the FT reactor and T is reactor temperature (K).

The given range of operating conditions are H_2/CO ratio from 0.5 to 4 and temperature from 423 K to 803 K¹⁷. In the rest of this paper this value for α is denoted α_2 .

3.3. Constant α (α_3)

A constant α of 0.9 is frequently proposed in the literature at typical operating conditions of a low temperature Cobalt based FT slurry bubble column reactor^{18,19}. We call this value $\alpha_3 = 0.9$.

4. Single-pass Fischer Tropsch reactor

We simulated the FT reactor individually (single pass) with only CO and H_2 in the feed, and show in Figures 5, 6 and 7 how the product distribution depends on the feed $\frac{H_2}{CO}$ ratio with models α_1 , α_2 and α_3 for the chain growth probability. The operating pressure and temperature for the reactor are assumed to be 2000 kPa and 210°C. Table 1 shows the corresponding conversion rates of CO, H_2 and production rates of methane and other hydrocarbons for $\frac{H_2}{CO} = 2$.

Table 1- FT reactor performance at $\frac{H_2}{CO} = 2$ feed when α_1 , α_2 or α_3 is used

Parameter	α_1	α_2	α_3
CO conversion, %	83.56	86.52	86.97
H_2 conversion, %	90.98	91.82	91.97
CH ₄ formation (kg/kg _{cat} .hr)	0.0106	0.011	0.011
Other hydrocarbons formation (kg/kg _{cat} .hr)	0.1877	0.1924	0.1924

In Figure 8, the value of α (α_1 , α_2 and α_3) is given as a function of $\frac{H_2}{CO}$. We see that α_2 is generally significantly higher than α_1 . α_2 is closest to the commonly used value of $\alpha_3 = 0.9$ and in addition the trend in Figure 6 (α_2) seems more realistic than Figure 5 (α_1). However, we will use both functions and also the constant α assumption in the following optimization.

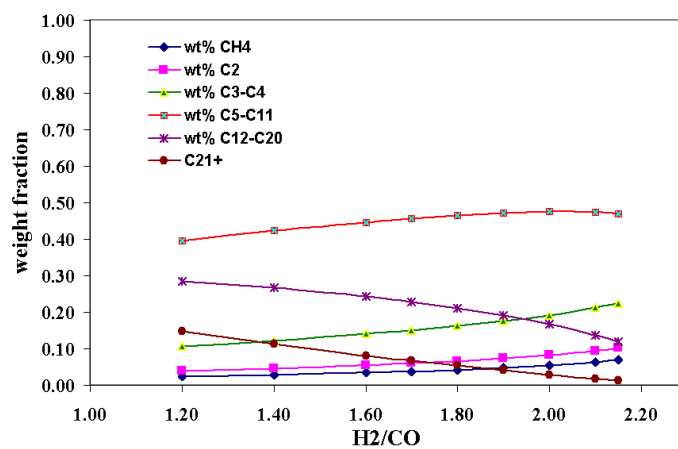


Fig. 5- FT reactor product distribution with α_1 from Iglesia reaction rates

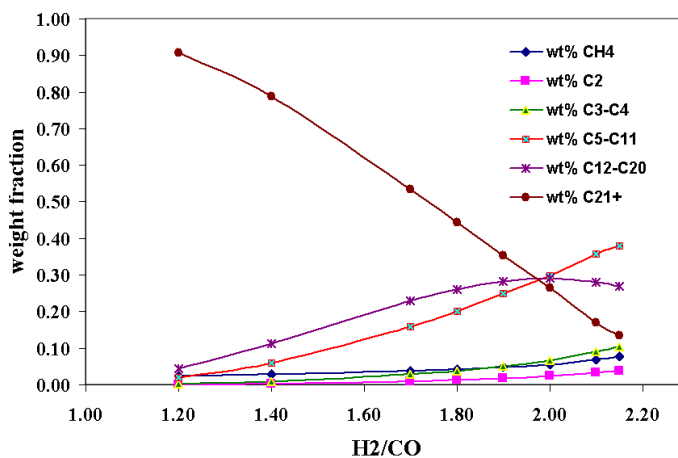


Fig. 6- FT reactor product distribution with α_2 from Yermakova and Anikeev

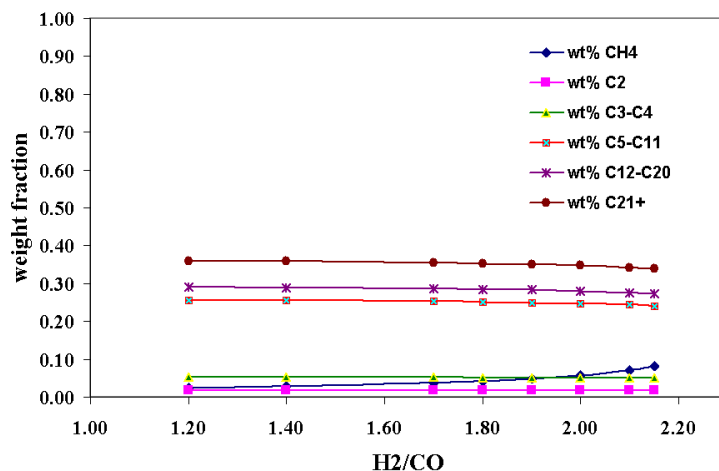


Fig. 7- FT reactor product distribution with $\alpha_3 = 0.9$

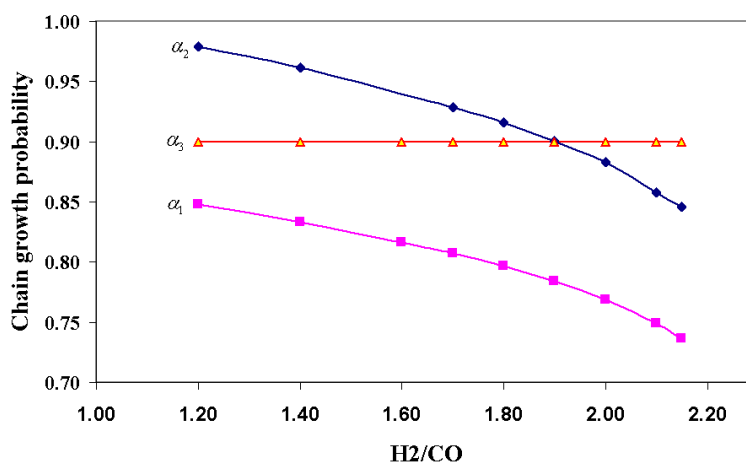


Fig. 8- Chain growth probability (α) as a function of $\frac{H_2}{CO}$ (feed) for different α models

5. Definition of optimal operation for overall process

The operational objective is to maximize the variable income (operational profit) with respect to the operational degrees of freedom subject to satisfying the constraints. Each of these is defined next.

5.1. Objective function

The objective function to be maximized is:

$$\text{Variable income (P)} = \text{sales revenue} - \text{variable cost} \quad (14)$$

The natural gas feedrate to the process side is fixed at 8195 kmol/h, but note that the natural gas used as fuel in the fired heater will vary, mainly depending on the amount and composition of the purged tail gas.

Sales revenue

We use the average price over the last 4 years in the Rotterdam market for Gasoline, Diesel and Fuel oil²⁰. The wax price is set equal to the fuel oil price. For LPG there is a large price variation depending on specifications and location, and an average price of the selling prices in different countries has been assumed.

This gives the following prices: LPG (C₃-C₄) = $0.9 \frac{\text{USD}}{\text{kg}}$, Gasoline/Naphtha (C₅-C₁₁) = $0.73 \frac{\text{USD}}{\text{kg}}$,

Diesel (C₁₂-C₂₀) = $0.71 \frac{\text{USD}}{\text{kg}}$, Wax (C₂₁₊) = $0.39 \frac{\text{USD}}{\text{kg}}$.

Variable cost

Variable cost = cost of raw materials + cost of energy + cost of CO₂ removal (15)

The raw materials are natural gas, water (steam) and oxygen.

- Natural gas price: $0.5 \frac{\text{USD}}{\text{MMbtu}}$ ²¹ with our gas composition this corresponds to $0.023 \frac{\text{USD}}{\text{kg}}$.

- CO₂ removal cost: $50 \frac{\text{USD}}{\text{ton CO}_2}$ ²²

- Water: cost set to zero.

- Energy: cost set to zero (assume excess energy available). Also, we did not include any credit for the “extra” saturated medium-pressure steam generated by the ATR hot effluent.

- Oxygen: It is assumed that the GTL plant must supply the required superheated steam for the oxygen plant, and in addition pay for the used oxygen with a price that decreases somewhat with increased oxygen usage.

$$P_{O_2} = P_{O_2}^o \left(\frac{\dot{m}_{O_2}}{\dot{m}_{O_2}^{ref.}} \right)^{-0.3}, P_{O_2}^o = 0.11 \frac{\text{USD}}{\text{kg O}_2} \quad (16)$$

The price policy makes the income for the O₂ plant less dependent on the operation in the GTL plant and also encourages the GTL plant to use more oxygen. The exponent of -0.3 implies that the oxygen price decreases by a factor of 2 if we use ten times more oxygen.

The capacity of the reference oxygen plant at $43.82 \frac{\text{kg}}{\text{sec}}$ is estimated based on the data from Holdor Topsøe^{3,23}.

5.2. Operational Degrees of freedom (steady-state)

The overall plant has 6 operational degrees of freedom at steady-state which can be chosen as the following. The chosen degrees of freedom are the ones, which have significant effect on objective function value and their optimal value is not clear from process understanding. The temperature for the FT reactor is assumed fixed at 210°C. The FT reactor operating pressure is assumed constant at 20 bar, which is the assumed maximum pressure for the reactor due to material constraints.

1- $\frac{H_2O}{C(\text{hydrocarbon})}$ (fresh + recycled),

2- $\frac{O_2}{C(\text{hydrocarbon})}$ (into ATR),

3- Fired heater duty,

4- CO₂ recovery percentage,

5- Purge ratio,

6- Recycle ratio to FT reactor

5.3. Operational constraints

We consider the following constraints during the optimization;

1. Molar ratio $\frac{H_2O}{C} \geq 0.3$ in feed to syngas unit. This is to avoid soot formation in the ATR. Haldor Topsøe reports³ soot free pilot operation at $\frac{H_2O}{C}$ ratios even as low as 0.2 but we conservatively use a lower bound of 0.3.
2. ATR exit temperature $\leq 1030^\circ C$. This temperature is an average of some the reported operating outlet ATR temperatures by Haldor Topsøe that ensures soot-free operation³.
3. Inlet temperature to ATR $\leq 675^\circ C$. This is a material constraint²⁴.
4. The purge ratio is optimally around 2% but for simulation purposes (to avoid convergence problem) it has bounded at a higher value (5% for α_1 model and 3% for α_2 and α_3 models).

6. Optimization results

The optimization (maximize P with respect to the degrees of freedom and constraints) was repeated using the three different α models ((12), (13) and constant α). For each α model, two price scenarios for the final products are considered. The first is the one mentioned earlier and the second is when the price of the wax is assumed to be twice as high i.e. $0.78 \frac{USD}{kg}$.

The UniSim “Mixed” method is used for optimization. This method initially uses the BOX method which is based on the Downhill Simplex algorithm and then a SQP method to locate the final solution⁷.

The results are reported in Tables 2, 3 and 4. For models α_1 and α_3 there is almost no effect of the wax price. The results with α_2 model seem more reasonable because a quite large sensitivity to the wax prices is expected. The H_2 to CO ratio (both in fresh syngas and in inlet stream into the FT reactor) are compared as these usually are considered the main parameters in determining the product distribution of GTL processes. The carbon efficiency in the Tables is defined as the ratio of carbon in the products and carbon in the natural gas feed, including natural gas used as fuel in the fired heater.

Table 2- Optimal operation when model α_1 is used

Wax price scenario	$\frac{H_2O}{C}$ (fresh+recycle)	$\frac{O_2}{C}$ (into ATR)	CO ₂ recovery	Recycle to FT	Purge of tail gas	$\frac{H_2}{CO}$ fresh	$\frac{H_2}{CO}$ into FT	α_1	Carbon efficiency	Objective function (USD/hr)
0.39 $\frac{USD}{kg}$	0.9080	0.5185	97.51%	82.00%	5%	2.06	1.80	0.7747	70.00%	41667
0.78 $\frac{USD}{kg}$	0.8059	0.5150	93.24%	84.90%	5%	2.02	1.67	0.7849	70.33%	43037

Table 3- Optimal operation when model α_2 is used (recommended)

Wax price scenario	$\frac{H_2O}{C}$ (fresh+recycle)	$\frac{O_2}{C}$ (into ATR)	CO ₂ recovery	Recycle to FT	Purge of tail gas	$\frac{H_2}{CO}$ fresh	$\frac{H_2}{CO}$ into FT	α_2	Carbon efficiency	Objective function (USD/hr)
0.39 $\frac{USD}{kg}$	0.8036	0.5226	93.00%	73.50%	3%	2.19	2.22	0.83	72.23%	44292
0.78 $\frac{USD}{kg}$	0.5100	0.5283	46.00%	86.00%	3%	1.88	1.39	0.92	75.94%	54795

Table 4- Optimal operation with fixed $\alpha_3 = 0.9$

Wax price scenario	$\frac{H_2O}{C}$ (fresh+recycle)	$\frac{O_2}{C}$ (into ATR)	CO ₂ recovery	Recycle to FT	Purge of tail gas	$\frac{H_2}{CO}$ fresh	$\frac{H_2}{CO}$ into FT	α_3	Carbon efficiency	Objective function (USD/hr)
0.39 $\frac{USD}{kg}$	0.441	0.5047	90.78%	79.08%	3%	2.08	1.98	0.90	75.92%	38470
0.78 $\frac{USD}{kg}$	0.4406	0.5076	91.00%	77.08%	3%	2.07	1.97	0.90	75.87%	54680

In all cases, we get the following three optimally active constraints:

- The purge ratio is active at its minimum (5% for α_1 model and 3% for α_2 and α_3).
- The fired heater outlet temperature is active at the maximum, 675°C.

- 1
2
3 - The ATR outlet temperature is active at the maximum, 1030°C. Since the outlet
4
5 temperature of ATR is quite high (1030°C), the equilibrium assumption is
6
7 reasonable.
8
9

10 One can imagine that the fired heater outlet temperature is set by the fired heater duty,
11
12 and the ATR outlet temperature is set by the oxygen feedrate. This leaves three
13
14 unconstrained optimization degrees of freedom (H₂O/C feed ratio, recycle ratio to FT
15
16 reactor, and CO₂ recovery fraction), for which, the optimal values result from the
17
18 optimization. For each of these three degrees of freedom, controlled variables need to be
19
20 identified. This is the topic of ongoing work (in preparation).
21
22
23

24 We now use the α_2 model in a more detailed study using an average wax price of
25
26 0.63 $\frac{\text{USD}}{\text{kg}}$. The results of the optimization for this case are shown in Table 5.
27
28
29
30
31
32

33 **Table 5- Optimal nominal values (α_2 model), wax price=0.63 $\frac{\text{USD}}{\text{kg}}$**

$\frac{\text{H}_2\text{O}}{\text{C}}$ (fresh+recycle)	$\frac{\text{O}_2}{\text{C}}$ (into ATR)	CO ₂ recovery	Recycle to FT	Purge of tail gas	$\frac{\text{H}_2}{\text{CO}}$ fresh	$\frac{\text{H}_2}{\text{CO}}$ into FT	α_2	Carbon efficiency	Objective function (USD/hr)
0.6389	0.5233	75.76%	76.83%	3%	2.1	2.01	0.87	74.24%	48402

34
35
36
37
38
39
40
41 Figure 9 shows the dependency of the profit function with respect to the six degrees of
42
43 freedom around the nominal optimal point. It shows that the profit value is sensitive to
44
45 change in the active constraints; purge ratio (Figure 9d), ATR inlet and outlet
46
47 temperatures (Figure 9e and 9f). The unconstrained degrees of freedom; $\frac{\text{H}_2\text{O}}{\text{C}}$ (Figure 9a)
48
49 and tail gas recycle ratio to FT (Figure 9b) have also significance effect on the objective
50
51 function while the objective function is almost flat with respect to the change in CO₂
52
53 recovery (Figure 9c).
54
55
56
57
58
59
60

1
2
3 The amount of light hydrocarbons carried along with the recycle vapor stream leaving the
4 three-phase separator depends on the conversion in the FT reactor, the H₂/CO ratio at the
5 outlet of syngas unit and chain growth probability. For example, in the nominal case the
6 tail gas composition on molar basis is: CH₄: 35.87%, H₂:21.42%, CO: 14.54%, N₂:
7 11.73%, CO₂: 8.38%, H₂O: 0.24% and other hydrocarbons: 7.82%.

8
9
10 The CH₄ in the tail gas should be recycled to the syngas unit, whereas the un-reacted CO
11 and H₂ should be recycled to FT reactor for further conversion, while the inert N₂ should
12 be purged. The optimal values for recycle and purge are determined by the optimization
13 as shown in Table 5. Note that there is no constraint on the inert fraction. The recycled
14 tail gas to the syngas unit needs to be compressed to 30 bar (Compressor in Figure 2).
15 The compressor work duty is only 1.15 MW, which is small compared to the fired heater
16 duty of 326 MW (thermodynamically, the equivalent work is about 54 MW) .

17
18
19 We will use this model for our future study to find the best controlled variables and
20 propose control structure in a systematic manner for different operational regions. In
21 addition, economical studies including consideration of different configurations of syngas
22 unit, CO₂ removal location etc. will be considered.
23
24
25
26
27
28
29
30
31
32
33
34
35
36
37
38
39
40
41
42
43
44
45
46
47
48
49
50
51
52
53
54
55
56
57
58
59
60

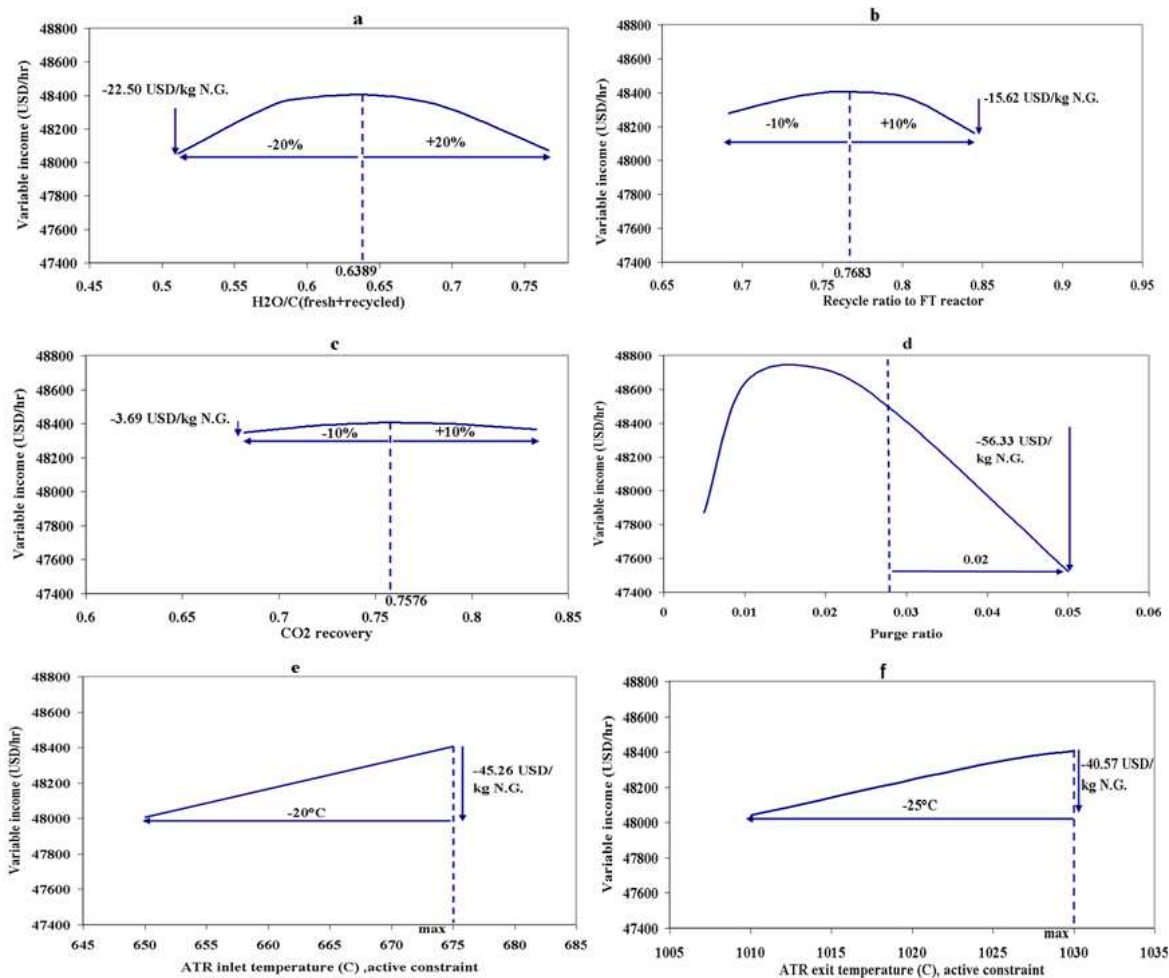


Fig. 9- Dependency of the variable income with respect to the decision variables and active constraints around optimal nominal point (nominal data from Table 5)

7. Conclusion

A gas to liquids process (GTL) has been simulated and optimized to describe the effect of decision variables on the plant variable income. Auto-thermal reforming (ATR) was chosen for syngas production and a Cobalt based slurry bubble column reactor was simulated using proposed Fischer-Tropsch reaction rates by Iglesia et al. Three different criteria for Fischer-Tropsch products distribution have been considered and the one proposed by Yermakova and Anikeev can very well describe dependencies in the overall process. The achieved model will be used for further control and economical studies.

Acknowledgment

The authors gratefully thank Dr. Dag Schanke (GTL specialist) at Statoil R&D center in Trondheim for his valuable discussions, comments and helping in design and simulation of the process.

Appendix

The proposed reaction rates by Iglesia et al. are as below¹⁴:

$$r_{CH_4} = \frac{1.08 \times 10^{-8} P_{H_2} P_{CO}^{0.05}}{1 + 3.3 \times 10^{-5} P_{CO}} \left(\frac{mol_{CH_4}}{g\text{-atom surface metal. s}} \right) \quad (\text{A-1})$$

$$r_{CO} = \frac{1.96 \times 10^{-8} P_{H_2}^{0.6} P_{CO}^{0.65}}{1 + 3.3 \times 10^{-5} P_{CO}} \left(\frac{mol_{CO}}{g\text{-atom surface metal. s}} \right) \quad (\text{A-2})$$

To convert these values to more common units, the following assumptions are made²⁵;

- The catalyst density is 2000 kg/m³,
- The weight fraction of Cobalt in the catalyst is 20% and 10% of the Cobalt is exposed as surface atoms,
- The catalyst volume fraction in the reactor is 10 %.

This gives the following values for r_{CO} and r_{CH_4} :

$$r_{CO} = \frac{1.96 \times 10^{-8} P_{H_2}^{0.6} P_{CO}^{0.65}}{1 + 3.3 \times 10^{-5} P_{CO}} \left(\frac{mol_{CO}}{g\text{-atom surface metal. s}} \right) \times \left(\frac{0.1g\text{-atom surface metal}}{mol_{Co\text{-total}}} \right) \times \left(\frac{1mol_{Co\text{-total}}}{58.9gr_{Co\text{-total}}} \right) \times \left(\frac{0.2gr_{Co\text{-total}}}{gr_{Cat.}} \right) \times \left(\frac{2000 \times 10^3 gr_{cat.}}{m_{cat.}^3} \right) \times \left(\frac{0.10m_{cat.}^3}{m_{reactor}^3} \right) \times \left(\frac{1kmol_{CO}}{1000mol_{CO}} \right) = \frac{1.331 \times 10^{-9} P_{H_2}^{0.6} P_{CO}^{0.65}}{1 + 3.3 \times 10^{-5} P_{CO}} \left(\frac{kmol_{CO}}{m_{reactor}^3 \cdot s} \right) \quad (\text{A-3})$$

$$r_{CH_4} = \frac{1.08 \times 10^{-8} P_{H_2} P_{CO}^{0.05}}{1 + 3.3 \times 10^{-5} P_{CO}} \left(\frac{mol_{CH_4}}{g\text{-atom surface metal. s}} \right) \times \left(\frac{0.1g\text{-atom surface metal}}{mol_{Co\text{-total}}} \right) \times \left(\frac{1mol_{Co\text{-total}}}{58.9gr_{Co\text{-total}}} \right) \times \left(\frac{0.2gr_{Co\text{-total}}}{gr_{Cat.}} \right) \times \left(\frac{2000 \times 10^3 gr_{cat.}}{m_{cat.}^3} \right) \times \left(\frac{0.10m_{cat.}^3}{m_{reactor}^3} \right) \times \left(\frac{1kmol_{CH_4}}{1000mol_{CH_4}} \right) = \frac{7.334 \times 10^{-10} P_{H_2} P_{CO}^{0.05}}{1 + 3.3 \times 10^{-5} P_{CO}} \left(\frac{kmol_{CH_4}}{m_{reactor}^3 \cdot s} \right) \quad (\text{A-4})$$

Selectivity to different hydrocarbons in FT reactions is described by well-known ASF

ideal model as (A-5):

$$w_n = n(1 - \alpha)^2 \alpha^{n-1} \quad (\text{A-5})$$

where w_n is the weight fraction of C_n and α is chain growth probability. Note that w_n is fraction of carbon atoms reacted totally which ends up in product with n C-atoms. This is almost (which is assumed here) but not completely the same as weight fraction²⁵.

Based on mass balance:

mass of consumed carbon as CO = mass of produced carbons (C_n) as FT products

The rate of CO consumption is correlated with weight fraction of the produced hydrocarbons as (A-6).

$$r_{CO} \left(\frac{kmol_{CO}}{m^3 \cdot hr} \right) \times \frac{12kg_C}{1kmol_{CO}} \times FT \text{ reactor volume}(m^3) = w_1 \left(\frac{kg_{CH_4}}{kg_{total \text{ hydrocarbons}}} \right) \times W_{total} (kg_{total \text{ hydrocarbons}} / hr) \times \frac{12kg_C}{16kg_{CH_4}} +$$

$$W_{total} (kg_{total \text{ hydrocarbons}} / hr) \times \left[w_2 \left(\frac{kg_{C_2H_6}}{kg_{total \text{ hydrocarbons}}} \right) \times \frac{1}{1+\gamma} \times \frac{2 \times 12kg_C}{30kg_{C_2H_6}} + w_2 \left(\frac{kg_{C_2H_4}}{kg_{total \text{ hydrocarbons}}} \right) \times \frac{\gamma}{1+\gamma} \times \frac{2 \times 12kg_C}{28kg_{C_2H_4}} \right] +$$

$$W_{total} (kg_{total \text{ hydrocarbons}} / hr) \times \left[w_3 \left(\frac{kg_{C_3H_8}}{kg_{total \text{ hydrocarbons}}} \right) \times \frac{1}{1+\gamma} \times \frac{3 \times 12kg_C}{44kg_{C_3H_8}} + w_3 \left(\frac{kg_{C_3H_6}}{kg_{total \text{ hydrocarbons}}} \right) \times \frac{\gamma}{1+\gamma} \times \frac{3 \times 12kg_C}{42kg_{C_3H_6}} \right] +$$

$$\dots +$$

$$W_{total} (kg_{total \text{ hydrocarbons}} / hr) \times \left[w_{20} \left(\frac{kg_{C_{20}H_{42}}}{kg_{total \text{ hydrocarbons}}} \right) \times \frac{1}{1+\gamma} \times \frac{20 \times 12kg_C}{282kg_{C_{20}H_{42}}} + w_{20} \left(\frac{kg_{C_{20}H_{40}}}{kg_{total \text{ hydrocarbons}}} \right) \times \frac{\gamma}{1+\gamma} \times \frac{20 \times 12kg_C}{280kg_{C_{20}H_{40}}} \right] +$$

$$W_{total} (kg_{total \text{ hydrocarbons}} / hr) \times \left[w_{25} \left(\frac{kg_{C_{25}H_{52}}}{kg_{total \text{ hydrocarbons}}} \right) \times \frac{1}{1+\gamma} \times \frac{25 \times 12kg_C}{352kg_{C_{25}H_{52}}} + w_{25} \left(\frac{kg_{C_{25}H_{50}}}{kg_{total \text{ hydrocarbons}}} \right) \times \frac{\gamma}{1+\gamma} \times \frac{25 \times 12kg_C}{350kg_{C_{25}H_{50}}} \right]$$

$$\text{where } w_{25} = (1 - w_1 - w_2 - \dots - w_{20}) \quad (A-7)$$

and γ is Olefin to Paraffin ratio. 20 reactions (C_1 - C_{20}) for paraffins and 19 reactions for Olefins (C_2 - C_{20}) are defined with weight fraction of w_n and the rest of the hydrocarbons are estimated with C_{25} as Wax (C_{21+}) with weight fraction of w_{25} . Simplification of eq.(A-6) yields weight of total hydrocarbons ($kg_{total \text{ hydrocarbons}} / hr$) in the product as eq.(A-8).

We choose reactor volume=2000m³ which gives reasonable CO and H₂ conversion in our model.

$$W_{total} (kg_{total \text{ hydrocarbons}} / hr) = \frac{r_{CO} \times 2000}{\left[\frac{w_1}{16} + 2w_2 \left(\frac{1}{1+\gamma} \frac{1}{30} + \frac{\gamma}{1+\gamma} \frac{1}{28} \right) + \dots + 25w_{25} \left(\frac{1}{1+\gamma} \frac{1}{352} + \frac{\gamma}{1+\gamma} \frac{1}{350} \right) \right]} \quad (A-8)$$

By having w_{total} , production rates of all hydrocarbons (paraffins and olefins) can be described as below.

$$r_{CH_4} = \frac{w_1 \times W_{total}}{16} \times \frac{1}{1+\gamma} = \frac{w_1}{30 \times [\frac{w_1}{16} + 2w_2(\frac{1}{1+\gamma} \frac{1}{30} + \frac{\gamma}{1+\gamma} \frac{1}{28}) + \dots + 25w_{25}(\frac{1}{1+\gamma} \frac{1}{352} + \frac{\gamma}{1+\gamma} \frac{1}{350})]} \times \frac{1}{1+\gamma} \times r_{CO} \times 2000 \quad (\text{A-9})$$

$$r_{C_2H_6} = \frac{w_2 \times W_{total}}{30} \times \frac{1}{1+\gamma} = \frac{w_2}{30 \times [\frac{w_1}{16} + 2w_2(\frac{1}{1+\gamma} \frac{1}{30} + \frac{\gamma}{1+\gamma} \frac{1}{28}) + \dots + 25w_{25}(\frac{1}{1+\gamma} \frac{1}{352} + \frac{\gamma}{1+\gamma} \frac{1}{350})]} \times \frac{1}{1+\gamma} \times r_{CO} \times 2000 \quad (\text{A-10})$$

$$r_{C_2H_4} = \frac{w_2 \times W_{total}}{28} \times \frac{\gamma}{1+\gamma} = \frac{w_2}{28 \times [\frac{w_1}{16} + 2w_2(\frac{1}{1+\gamma} \frac{1}{30} + \frac{\gamma}{1+\gamma} \frac{1}{28}) + \dots + 25w_{25}(\frac{1}{1+\gamma} \frac{1}{352} + \frac{\gamma}{1+\gamma} \frac{1}{350})]} \times \frac{\gamma}{1+\gamma} \times r_{CO} \times 2000 \quad (\text{A-11})$$

...

$$r_{C_{25}H_{52}} = \frac{w_{25} \times W_{total}}{352} \times \frac{1}{1+\gamma} = \frac{(1 - w_1 - w_2 - \dots - w_{25})}{352 \times [\frac{w_1}{16} + 2w_2(\frac{1}{1+\gamma} \frac{1}{30} + \frac{\gamma}{1+\gamma} \frac{1}{28}) + \dots + 25w_{25}(\frac{1}{1+\gamma} \frac{1}{352} + \frac{\gamma}{1+\gamma} \frac{1}{350})]} \times \frac{1}{1+\gamma} \times r_{CO} \times 2000 \quad (\text{A-12})$$

$$r_{C_{25}H_{50}} = \frac{w_{25} \times W_{total}}{350} \times \frac{\gamma}{1+\gamma} = \frac{(1 - w_1 - w_2 - \dots - w_{25})}{350 \times [\frac{w_1}{16} + 2w_2(\frac{1}{1+\gamma} \frac{1}{30} + \frac{\gamma}{1+\gamma} \frac{1}{28}) + \dots + 25w_{25}(\frac{1}{1+\gamma} \frac{1}{352} + \frac{\gamma}{1+\gamma} \frac{1}{350})]} \times \frac{\gamma}{1+\gamma} \times r_{CO} \times 2000 \quad (\text{A-13})$$

γ (Olefins to Paraffins ratio) is assumed to be in average value of 0.35 for all hydrocarbons¹⁴.

References

- (1) Rostrup-Nielsen, J.; Dybkjaer, I.; Aasberg-Petersen, K. Synthesis gas for large scale Fischer-Tropsch synthesis. American Chemical Society, Division of Petroleum Chemistry, Preprints 2000, 45, 2, 186-189.
- (2) Steynberg, A. P.; Dry, M. E. Fischer Tropsch Technology. 2004; Vol. 152.
- (3) Aasberg-Petersen, K.; Christensen, T. S.; Stub Nielsen, C.; Dybkjær, I. Recent developments in autothermal reforming and pre-reforming for synthesis gas production in GTL applications. Fuel Processing Technology 2003, 83, 253-261.
- (4) Bakkerud, P. K. Update on synthesis gas production for GTL. Catalysis Today 2005, 106, 30-33.
- (5) Schijndel, J. v.; Thijssen, N.; Baak, G.; Avhale, A.; Ellepola, J.; Grievink, J. Development of a synthesis tool for Gas-To-Liquid complexes. Proceedings of 21st European Symposium on Computer Aided Process Engineering 2011, 417-421.
- (6) GTL-Workshop, Introduction to GTL Technology, Pre-Symposium Workshop. Organized by Gas Processing Center and Shell Company 2010, Doha, Qatar.
- (7) UniSim Design, R380, 2008, Honeywell Company.
- (8) Bao, B.; El-Halwagi, M. M.; Elbashir, N. O. Simulation, integration, and economic analysis of gas-to-liquid processes, Fuel Processing Technology 2010, 91, 7, 703-713.
- (9) Christensen, T. S. Adiabatic prereforming of hydrocarbons - an important step in syngas production. Applied Catalysis A: General 1996, 138, 2, 285-309.

- 1
2
3
4 (10) Schanke, D.; Sogge, J., Personal communication. Statoil research center/Trondheim,
5 2010.
6
7
8 (11) Cohen, H.; Rogers, G. F. C.; Saravanamuttoo, H. I. H., Gas turbine theory. 6th
9 edition, 2009.
10
11 (12) Aasberg-Petersen, K.; Bak Hansen, J. H.; Christensen, T. S.; Dybkjaer, I.;
12 Christensen, P. S.; Stub Nielsen, C.; Winter Madsen, S. E. L.; Rostrup-Nielsen, J. R.
13 Technologies for large-scale gas conversion. Applied Catalysis A: General 2001, 221,
14 379-387.
15
16
17 (13) Yates, I. C.; Satterfield, C. N. Intrinsic kinetics of the Fischer-Tropsch synthesis on a
18 Cobalt catalyst. Energy & Fuels 1991, 5, (1), 168-173.
19
20
21 (14) Iglesia, E.; Reyes, S. C.; Soled, S. L. Reaction-Transport selectivity models and the
22 design of fischer-tropsch catalysts. Computer-aided design of catalysts, Becker R. E. ;
23 Pereira. C. J. eds.,1993;199-257.
24
25 (15) Spath, P. L.; Dayton, D. C. Preliminary Screening Technical and Economic
26 Assessment of Synthesis Gas to Fuels and Chemicals with Emphasis on the Potential for
27 Biomass-Derived Syngas, [http://www.fischer-tropsch.org/DOE/DOE_reports/510/510-](http://www.fischer-tropsch.org/DOE/DOE_reports/510/510-34929/510-34929.pdf)
28 [34929/510-34929.pdf](http://www.fischer-tropsch.org/DOE/DOE_reports/510/510-34929/510-34929.pdf) .
29
30
31 (16) Yermakova, A.; Anikeev, V. I., Thermodynamic Calculations in the Modeling of
32 Multiphase Processes and Reactors. Industrial & Engineering Chemistry Research 2000,
33 39, 5, 1453-1472.
34
35 (17) Song, H.-S.; Ramkrishna, D.; Trinh, S.; Wright, H. Operating strategies for Fischer-
36 Tropsch reactors: A model-directed study. Korean Journal of Chemical Engineering
37 2004, 21, 2, 308-317.
38
39
40 (18) Jager, B.; Espinoza, R., Advances in low temperature Fischer-Tropsch synthesis.
41 Catalysis Today 1995, 23, 1, 17-28.
42
43 (19) Satterfield, C. N.; Yates, I. C.; Chanenchuk, C.; DOE Report no. PC79816-6,
44 Contract no. DE-AC22-87PC79816, July-September.; 1989.
45
46
47 (20) OPEC, Annual Statistical Bulletin, www.opec.org. 2009.
48
49 (21) Halstead, K., Oryx GTL: a case study, details the first new generation commercial
50 scale gas to liquids plant; Foster Wheeler.
51 www.fwc.com/publications/tech_papers/files/Oryx781fosterwheeler.pdf
52
53
54 (22) ZEP Report CO₂ Capture Costs, ZEP Capture Cost Working Group; European
55 Technology Platform for Zero Emission Fossil Fuel Power Plants, Report 2011.
56
57
58
59
60

1
2
3 (23) Dybkjær, I. Synthesis Gas Technology. Preprinted from hydrocarbon engineering
4 July2006.

5 [http://www.topsoe.com/business_areas/synthesis_gas/~media/PDF%20files/Heat_excha](http://www.topsoe.com/business_areas/synthesis_gas/~media/PDF%20files/Heat_exchange_reforming/Topsoe_synthesis_gas_technology.ashx)
6 [nge_reforming/Topsoe_synthesis_gas_technology.ashx](http://www.topsoe.com/business_areas/synthesis_gas/~media/PDF%20files/Heat_exchange_reforming/Topsoe_synthesis_gas_technology.ashx)

7
8 (24) Bakkerud, P. K., Personal Communication. Haldor Topsøe, 2009.

9
10 (25) Schanke, D., Personal Communication. Statoil research center/Trondheim, 2010.
11
12
13
14
15
16
17
18
19
20
21
22
23
24
25
26
27
28
29
30
31
32
33
34
35
36
37
38
39
40
41
42
43
44
45
46
47
48
49
50
51
52
53
54
55
56
57
58
59
60

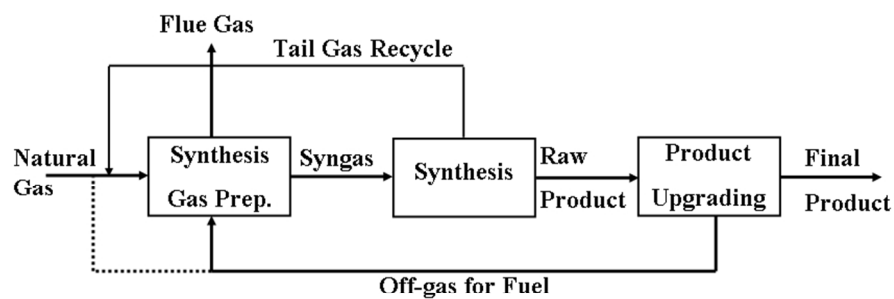
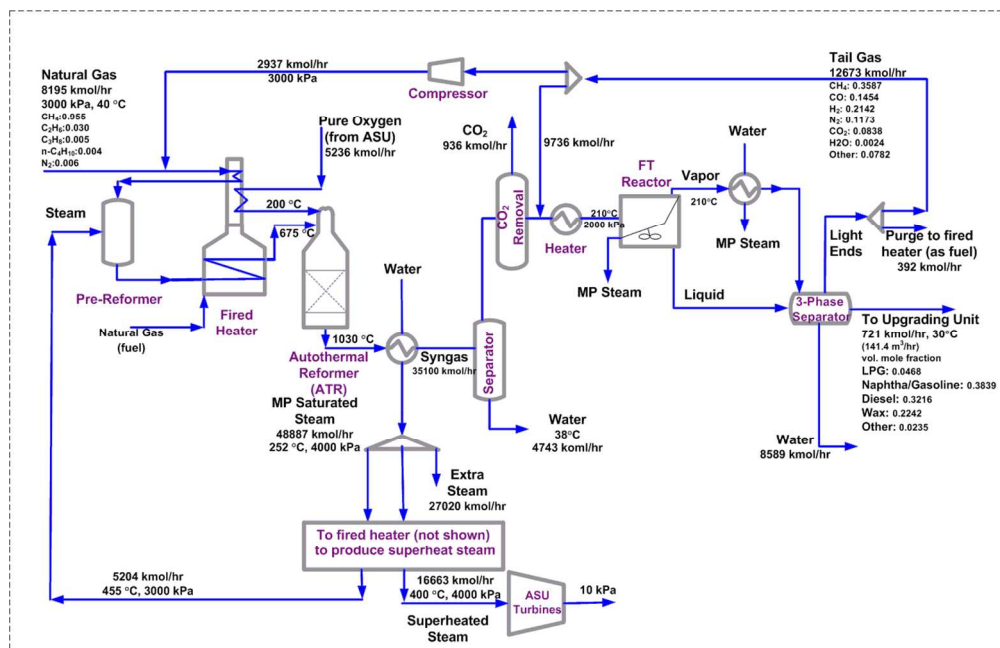
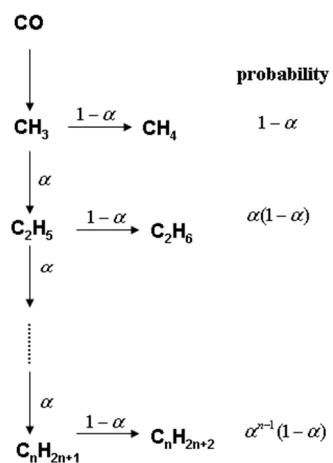


Fig. 1- A simple Flowsheet of a GTL process1
254x190mm (96 x 96 DPI)



366x235mm (96 x 96 DPI)



32 Fig. 3- Probability of chain growth to different hydrocarbons in FT reactions6
33 254x190mm (96 x 96 DPI)

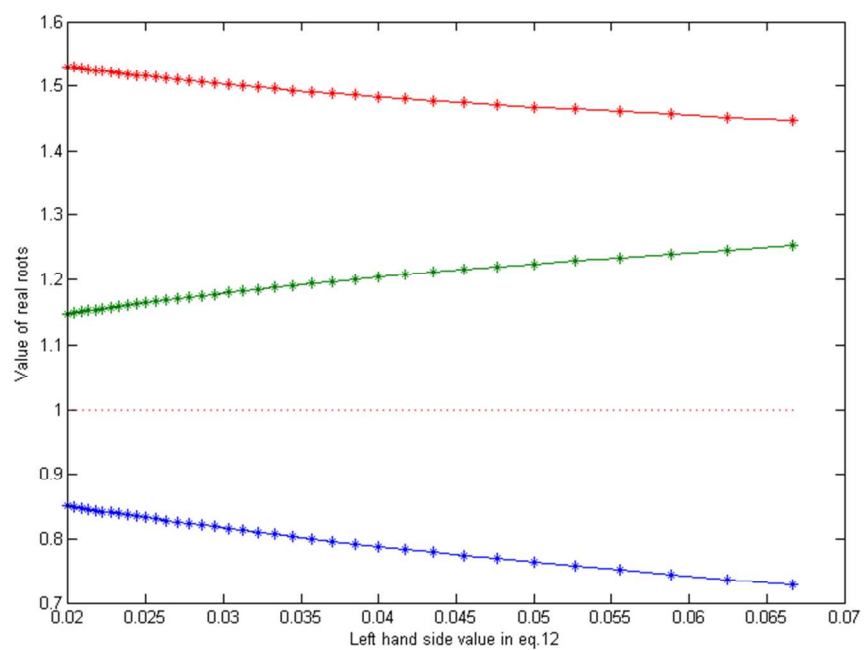


Fig. 4- Real roots as a function of the selectivity ($1.2 \leq H_2/CO \leq 2.15$)
207x148mm (96 x 96 DPI)

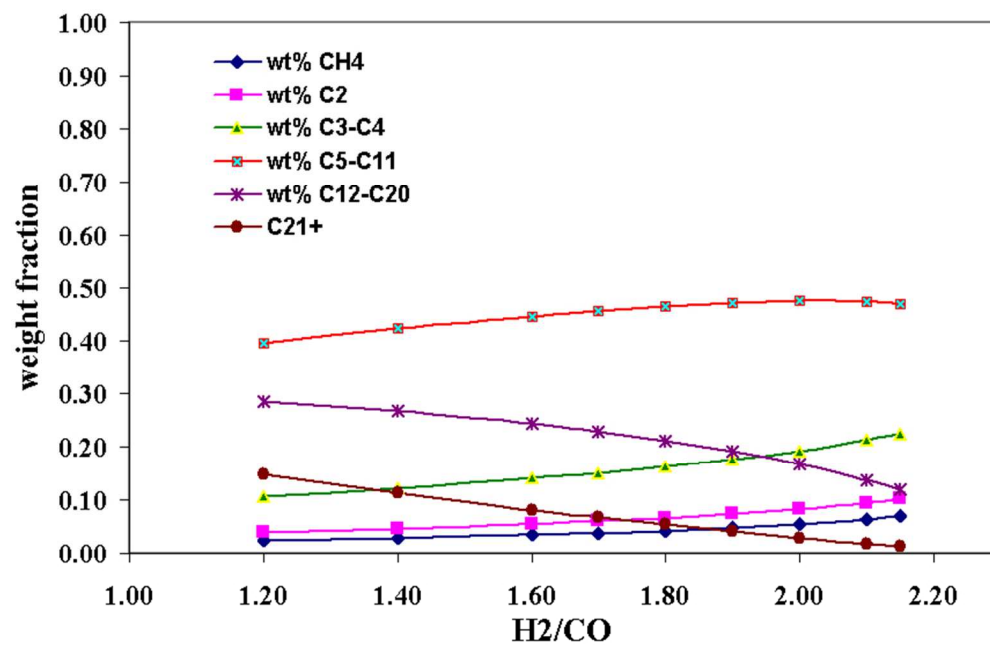


Fig. 5- FT reactor product distribution with from Iglesia reaction rates
228x148mm (96 x 96 DPI)

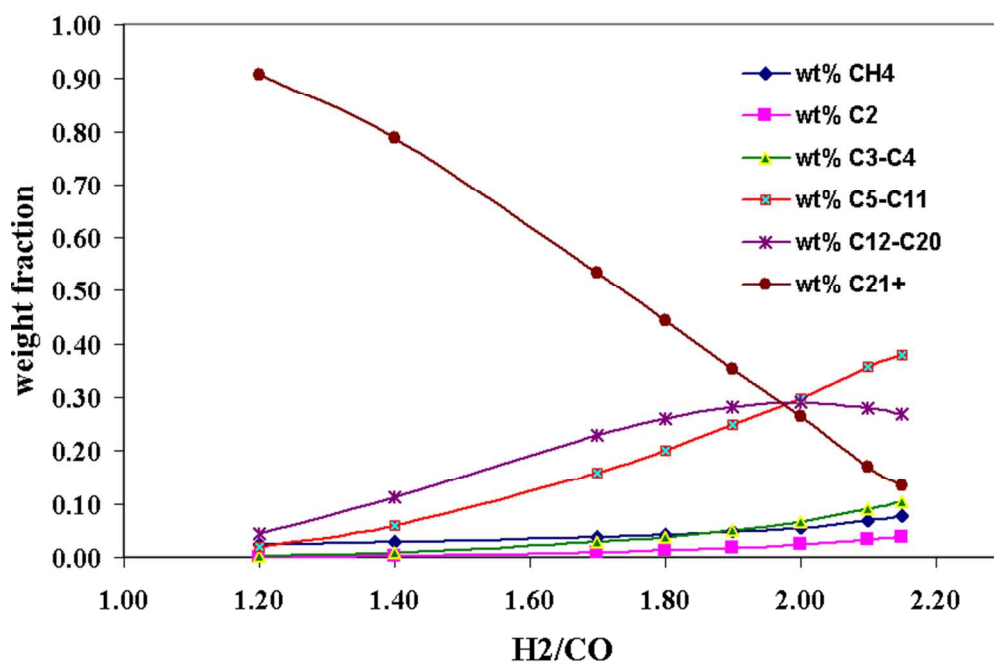


Fig. 6- FT reactor product distribution with from Yermakova and Anikeev
225x151mm (96 x 96 DPI)

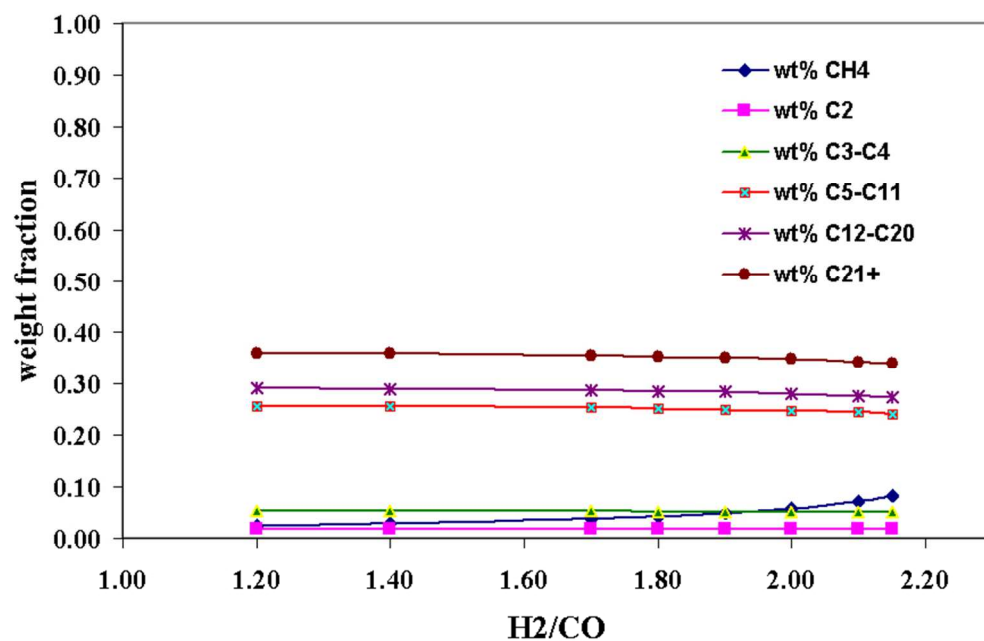


Fig. 7- FT reactor product distribution with
233x151mm (96 x 96 DPI)

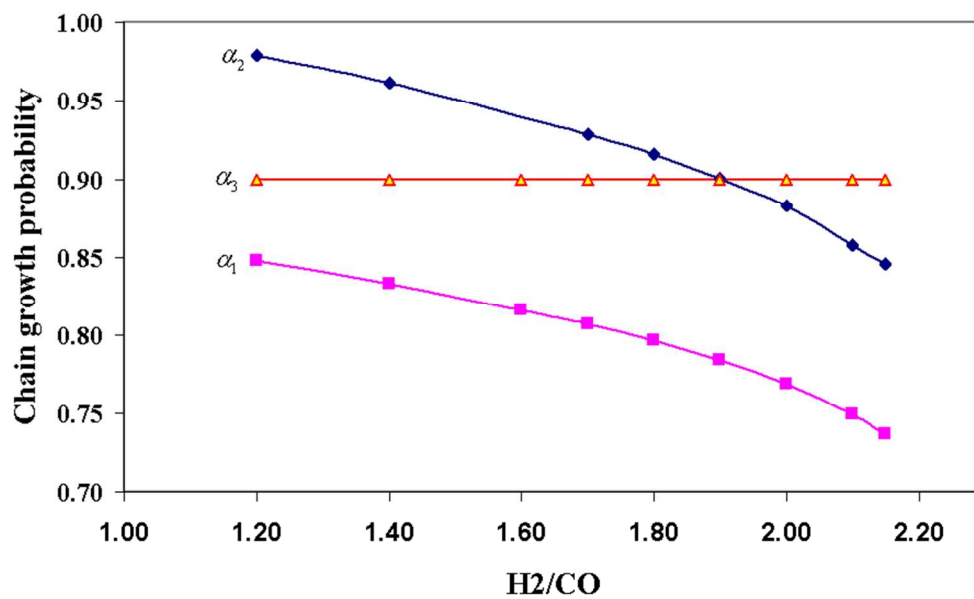


Fig. 8- Chain growth probability () as a function of (feed) for different models
241x145mm (96 x 96 DPI)

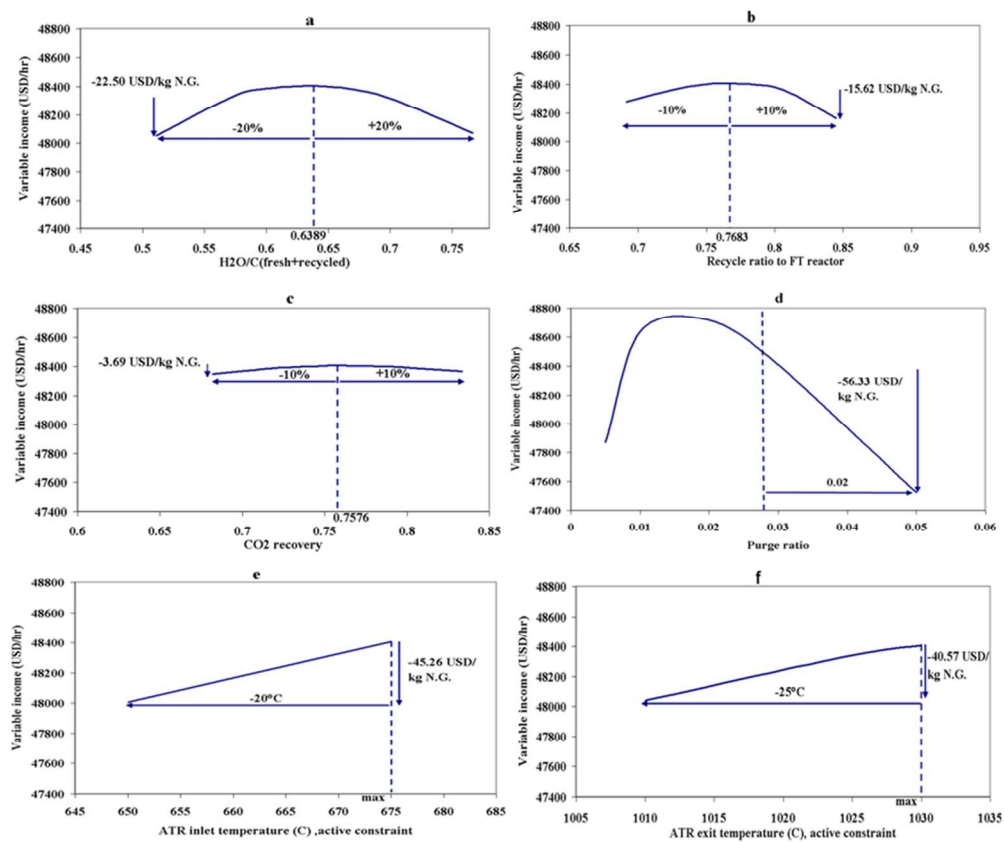


Fig. 9- Dependency of the variable income with respect to the decision variables and active constraints around optimal nominal point (nominal data from Table 5)
231x195mm (96 x 96 DPI)